Dynamos in Stellar Convection Zones: of Wreaths and Cycles[1]

Benjamin Brown

Dept. of Astronomy and Center for Magnetic Self Organization in Laboratory and Astrophysical Plasmas, University of Wisconsin, Madison, WI 53706, USA

E-mail: bpbrown@astro.wisc.edu

Abstract. We live near a magnetic star whose cycles of activity are driven by dynamo action beneath the surface. In the solar convection zone, rotation couples with plasma motions to build highly organized magnetic fields that erupt at the surface and undergo relatively regular cycles of polarity reversal. Despite our proximity to the Sun, the nature of its dynamo remains elusive, but observations of other solar-type stars show that surface magnetism is a nearly ubiquitous feature. In recent time, numerical simulations of convection and dynamo action have taken tremendous strides forward. Global-scale organization and cyclic magnetism are being achieved by several groups in distinctly different solar and stellar simulations. Here I will talk about advances on the numerical front including wreath-building dynamos that may occupy stellar convection zones. I will discuss the interplay between the new simulations, various classes of mean-field models, and current and upcoming solar and stellar observations.

1. Introduction

The 22-year solar activity cycle stands out as one of the most remarkable and enigmatic examples of magnetic self-organization in nature. The magnetism we see at the surface as sunspots likely originates in the solar convection zone, where turbulent plasma motions couple with rotation and magnetic fields to drive strong dynamo action. Magnetism is a ubiquitous feature of solar-type stars and there are well known scaling relationships between the amount of surface magnetism and stellar properties, such as rotation rate and stellar-type [e.g., 1]. Other late-type stars undergo similar magnetic cycles, with periods ranging from several years to several decades [2, 3]. As in the case of the solar cycle, these must arise through hydromagnetic dynamos operating in their convective envelopes. However, the observational landscape is complex, with few well-established trends to constrain dynamo models [e.g., 4, 5].

Indeed, explaining the origin of globally organized fields and cyclic behavior in the Sun has inspired and challenged astrophysical dynamo theory for over a century and continues to do so. The tremendous growth of computational resources, coupled with the insights afforded by helioseismology about the solar internal structure and differential rotation, has lead to an explosion of dynamo modeling efforts. These range from sophisticated 2D mean-field models that incorporate data assimilation techniques to fully 3D simulations that can capture non-linear dynamics of solar convection and self-consistently establish solar-like differential rotation profiles. Both classes of models are being applied to stars other than the Sun, sampling different spectral types and exploring how rotation affects stellar convection and dynamo action.

[1] proceedings for SOHO 24/GONG 2010 conference: "A new era of seismology of the Sun and solar-like stars," Aix-en-Provence, France, June 27-July 4, 2010 (JPCS)

Here I will briefly review the state of dynamos for the Sun and sun-like stars that rotate somewhat faster, as the Sun did in its youth. These studies are suggesting new modes of global-scale dynamo action and are raising exciting questions about the nature of the solar dynamo.

2. Mean-field models of stellar dynamos

Simulations of the solar dynamo and solar convection are generally broken into two classes: the two dimensional (2D) mean-field models and the three-dimensional (3D) simulations. By going to 2D, typically in radius and latitude, the computations can be made much more tractable and high resolution simulations can be pursued for very long intervals of time. It is not unusual for such models to simulate several tens of solar cycles, and reproducing the entire observational record of sunspots is quite feasible [e.g., 6].

The trouble lies in the treatment of turbulence and non-linear correlations. Dynamo action generally requires correlations between the non-axisymmetric, fluctuating velocity and magnetic fields. In mean-field models these non-axisymmetric flows are not directly simulated and instead must be captured through some assumed model. This is a very difficult and outstanding problem in turbulence theory. Generally, an attempt is made to model the coherent effect of the fluctuations in terms of the global-scale (mean) fields, and this is often embodied as an "α-effect," though many variations have been explored. Cyclonic convection coupling with rotation is often associated with the α-effect and thus α is thought typically to depend on the kinetic helicity of the convection, but the α-effect remains very difficult to constrain observationally. Comparable difficulties underlie descriptions of the turbulent processes that transport angular momentum to self-consistently establish the observed solar differential rotation. This mean internal rotation profile, however, can be measured in detail throughout the solar convection zone, and the observed profile is directly incorporated in the mean-field models [e.g., 7].

The α-effect is most important for the regeneration of poloidal (north-south) magnetic field; mean toroidal fields can be generated from a mean poloidal field by the shear of differential rotation in what is generally called an "Ω-effect." These $\alpha\Omega$ dynamos and their variants have become central to the language used to discuss solar and stellar dynamos. Some live in the convection zone alone while others rely on the interface at the base of the convection zone, the tachocline, to generate cyclic reversals of global-scale polarity.

Many recent solar dynamo models have also emphasized the meridional circulation as a potentially important factor in promoting cyclic magnetic activity [e.g., 6, 8–14]. In these *Flux-Transport* models, the equatorward migration of emerging bipolar active regions over the course of the solar cycle is attributed to the equatorward advection of toroidal flux in the lower convection zone by the mean circulation. Many Flux-Transport models are also *Babcock-Leighton* models whereby the principle source of mean poloidal field generation is the buoyant emergence and subsequent dispersal of fibril toroidal flux concentrations, often modeled as a non-local α-effect [15]. Although the physical origin of the Babcock-Leighton mechanism is distinct from the turbulent α-effect underlying distributed and interface dynamo models, the fields generated are still helical in nature and this helicity ultimately arises from the rotation of the star.

The review by Charbonneau [15] is an excellent place to read in more detail about these models, while [16] delves into the details of the turbulence models themselves. Comparisons between many of the codes used in different mean-field models have been undertaken by [17]. Mean-field models still do not unambiguously reproduce the solar cycle, despite heroic efforts leading up to the current cycle [e.g., 6]. To be clear, these models are much further along than the 3D models, which are beginning to regularly produce cyclic solutions only in recent time [e.g., 18–21]. Mean-field models can be run for many solar cycles and are an invaluable tool for exploring the extensive parameter space of solar and stellar convection, and several explorations have been made of global-scale circulations in solar-like stars [e.g., 22–26]. However, many of the important underlying variables are difficult to constrain (e.g., the dependence of α on radius

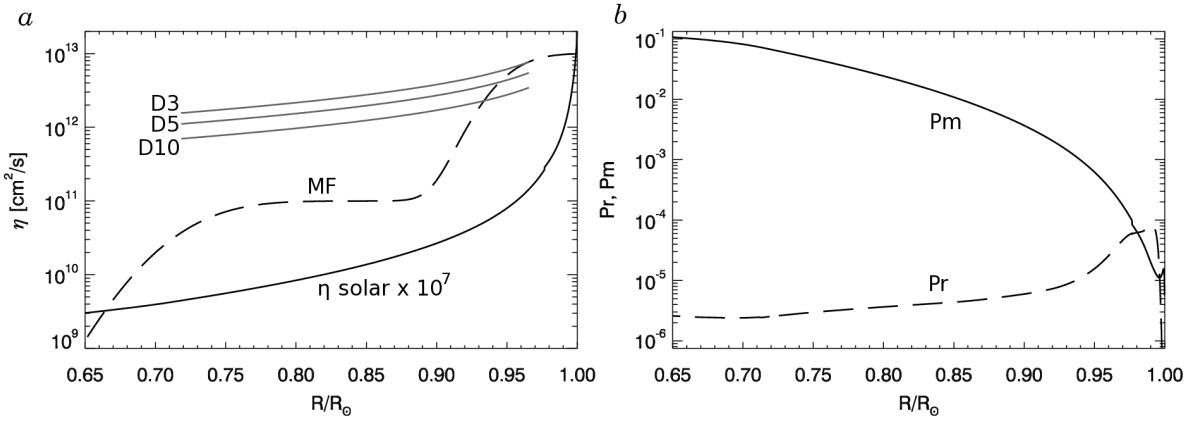

Figure 1. (a) Radial profiles of magnetic diffusivity η used in various models. Shown is the double-step profiles used in the Babcock-Leighton models of [7] and similar to that used in [6, 27] (MF,- - - -). Three profiles from 3D MHD ASH dynamos are shown for comparison; these correspond to cases D3, D5 and D10 (grey lines). The molecular diffusivity for a hydrogen plasma at solar conditions is also shown, multiplied by 10^7 for display purposes. (b) The Prandtl number $\mathrm{Pr} = \nu/\kappa$ (dashed) and magnetic Prandtl number $\mathrm{Pm} = \nu/\eta$ (solid) for a hydrogen plasma at solar conditions. Simulations use values of order unity.

and latitude in the Sun; how α varies with stellar properties such as rotation rate and mass; the applicability of α-effects to modeling the turbulent induction observed in 3D models; etc.). We turn now to a discussion of fully non-linear 3D convection driven dynamos, which are beginning to provide the opportunity to better constrain these unknown quantities.

3. The gap between simulations and the Sun

Numerical studies of the solar dynamo have a rich history, with the the first 3D magnetohydrodynamic (MHD) convective global-scale solar dynamo simulations attaining cyclic behavior in the early studies of Gilman [28]. Those Boussinesq simulations were quickly joined by fully non-linear global-scale anelastic simulations, which captured the stratified nature of the solar convection zone as well [29, 30]. Computational resources have grown at a tremendous rate, and with them the complexities of the models studied. Modern simulations typically have higher resolutions and evolve for longer intervals of time; in one simulation we will examine later (case D5), this represents roughly a factor of a million more computation than was possible in early studies [28]. This is is in surprisingly good agreement with Moore's law doubling over the almost thirty year interval separating these simulations, but it helps clarify the huge gap remaining between solar convection and the highest resolution simulations: another century of growth might provide the resources to directly simulate solar convection on global-scales.

Stellar convection spans a vast range of spatial and temporal scales which remain well beyond the grasp of direct numerical simulation. Models of stellar dynamos must make various tradeoffs, either building up from the diffusive scales or building down from the global-scales. These are respectively called *local* or *global* simulations; the latter will be our focus here. The highest resolution modern 3D simulations, running on massively parallel supercomputers, capture roughly 1000^3 total points and typically can evolve for some $10^6 - 10^7$ timesteps. In the Sun, the smallest scales of motion are set by diffusion and are likely of order 1 mm [e.g., review 31] while the largest scales or motion are comparable to the solar radius (700 Mm), with a total spectral range of almost 10^{12} in each of three dimensions. Temporal separations are similar, with fast granulation on the surface overturning on roughly five minute timescales while the deep structure of the Sun evolves over a span of gigayears.

Clearly, stellar dynamo studies must drastically simplify the physics of the stellar interior. Molecular values of the magnetic diffusivity η for a hydrogen plasma under the conditions of the the solar convection zone range from roughly 10^2–10^6 cm^2/s as one moves from the tachocline to the near surface regions, while the molecular viscosity ν is of order 10 cm^2/s in the solar convection zone [e.g., 32, 33]. These diffusivities are vastly smaller than the values used in either mean-field models or 3D MHD simulations, and we illustrate this in Figure 1.

In contrast to the solar values, simulations typically employ values of η and ν that are of order 10^{12} cm^2/s; this large value is more similar to simple estimates of turbulent diffusion associated with granulation at the surface where $\nu_{\rm t} \sim V_{\rm t} L_{\rm t} \sim 10^{11}$ cm^2/s given $V_{\rm t} \sim 1$ km/s and $L_{\rm t} \sim 1$ Mm [e.g., 31]. Shown in Figure 1*a* are radial profiles of η for both mean-field models and 3D MHD dynamo simulations with the ASH code. Mean-field models often match to a turbulent diffusion consistent with supergranulation at the surface and then taper to a lower value at mid-convection zone (here 10^{11} cm^2/s) [e.g., 6, 7, 27]. Below the tachocline, $\eta_{\rm MF}$ is tapered further, sometimes approaching the molecular values. In 3D models the choice is often made to scale η with the background density. Here a scaling of $\rho^{-0.5}$ is used, though in other studies the exponent can scale from 0 to -1 [e.g., 34]. The relative mixing from diffusion of vorticity (by viscosity ν), temperature (κ) and magnetism (η) is given by the Prandtl number and magnetic Prandtl number, which are shown in Figure 1*b*. Molecular ratios for a hydrogen solar plasma are tiny, with Pm ranging from 10^{-1} to 10^{-5} while Pr is of order 10^{-5}. Turbulent values are likely of order unity but are not well constrained under solar conditions; simulations typically take Pm and Pr to be near unity as resolving large separations in diffusive scales requires very high resolutions.

4. Convection driven dynamos: the Sun

Despite this daunting separation in parameter space, modern models are making tremendous strides in understanding the non-linear couplings between convection and rotation that build the solar differential rotation. It is now possible to study relatively high Reynolds number convection (fluctuating Re of order a few hundred) in stratified convection zones capturing density contrasts exceeding 100 (e.g., more than 5 density scale heights) between the base of the convection zone and the near-surface layers. The anelastic spherical harmonic (ASH) code has been a very useful tool in global-scale studies [34–36]; tremendous progress has been made in models of photospheric convection as well, but those will not be the focus here [e.g., 37].

Simulations of solar convection self-consistently produce solar-like profiles of differential rotation, with prograde equators, retrograde polar regions and a monotonic decrease of angular velocity with latitude. This profile is achieved partly through the redistribution of angular momentum by turbulent Reynolds stresses in the convection [38–40]. The differential rotation profile is in what is called a "thermal-wind balance", with an accompanying latitudinal gradient of temperature. This is an effect that is well known in the geophysical community, entering the vorticity evolution equation as a baroclinic term. In solar convection, thermal-wind balance leads to more conical profiles of angular velocity Ω [38, 40]. Simulations suggest that in the Sun the accompanying temperature perturbations at the solar surface may be of order 1-10K. Perturbations of this size at the base of the convection zone, consistent with the geostrophic balances likely achieved in the tachocline, can serve to tilt the contours of constant Ω until very good agreement is attained between simulations and helioseismic measurements [41, 42].

Solar dynamo simulations generally produce complex magnetic topologies, with more than 95% of the magnetic energy in the fluctuating (non-axisymmetric) field components [34]. Mean fields are complex, with multipolar structure and transient toroidal ribbons and sheets. Polarity reversals of the dipole component occur but they are irregular in time. The presence of an overshoot region and a tachocline of rotational shear promotes mean-field generation, producing persistent bands of toroidal flux antisymmetric about the equator while strengthening and

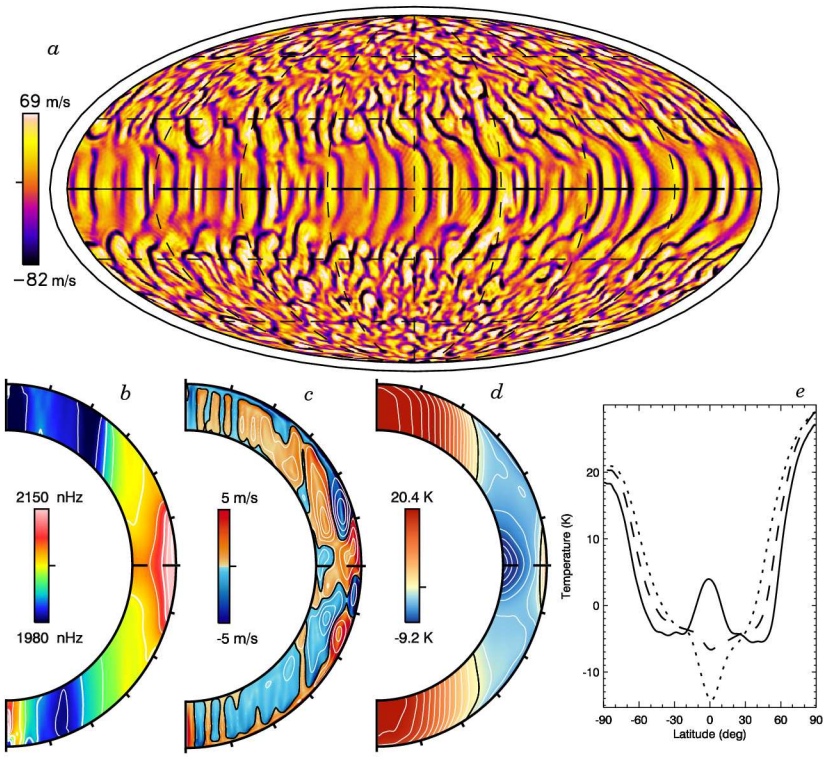

Figure 2. Convection and global-scale flows in case D5 [18]. (*a*) Convective patterns of radial velocity v_r in global Mollweide projection at 0.95 $R_\odot$ with upflows light and downflows dark. Poles are at top and bottom and thin line denotes stellar surface. (*b*) Differential rotation shown with longitudinally averaged angular velocity Ω. The rotation is solar-like, with fast (prograde) equator. (*c*) Meridional circulations with color indicating amplitude and sense of circulation (red counter-clockwise; blue clockwise) and mass flux streamlines overlaid. Compared to solar simulations, the circulations here are broken into several weaker cells in both radius and latitude. (*d*) Profile of mean temperature fluctuations. This profile, with hot poles and cool mid-latitudes, represents the thermal wind balance achieved with the differential rotation. (*e*) Latitude cuts of temperature at fixed radius, sampling top (——), middle (– – –) and bottom (· · · · · ·) of convection zone. At the surface, the temperature contrast in latitude can reach 30K. Profiles shown in *b*–*e* have been averaged in time over a 225 day interval.

stabilizing the dipole moment [43–45]. These simulations exhibit notable self-organization through the turbulent pumping of magnetic flux into the tachocline, amplification by rotational shear, and selective shear-induced dissipation of small-scale magnetic fluctuations. Modern simulations build organized magnetic fields and attain cyclic behavior, sometimes with a tachocline playing an important role [19, 20], and sometimes in the convection zone of the Sun alone [21, 46]. We now turn to the special class of wreath-building convection zone dynamos.

5. Convection driven dynamos: rapidly rotating suns

When stars like the Sun are younger they rotate much more rapidly. These stars are observed to have strong surface magnetic activity and are thought to have very active dynamos in their convection zones. Rotational constraints are stronger in more rapidly rotating systems and this can lead to greater correlations as convective structures align with the rotation axis.

Patterns of convection in a simulation of a young, rapidly rotating sun are shown in Figure 2*a* near the stellar surface. Convection fills the domain and near the equator is strongly north-south

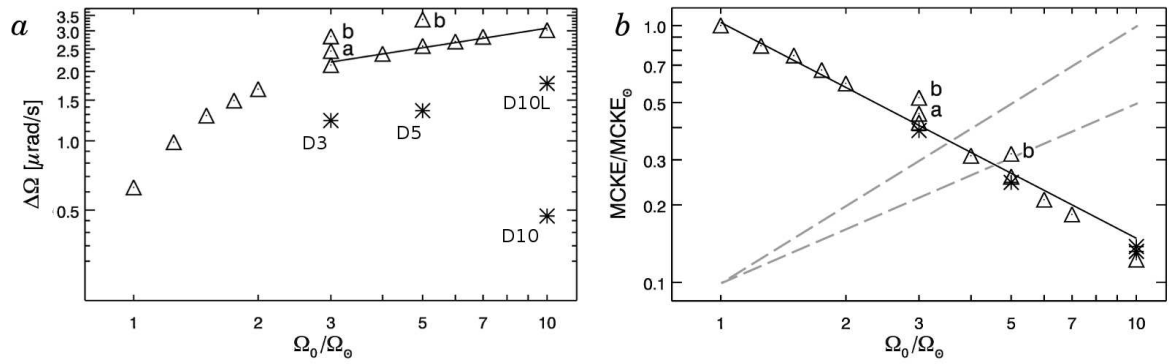

Figure 3. Global-scale flows and stellar rotation [47]. (*a*) Angular velocity shear of differential rotation $\Delta\Omega$ in latitude near the stellar surface shown as a function of rotation rate Ω_0 relative to the solar rotation rate $\Omega_\odot$. Hydrodynamic cases are shown with diamonds while dynamos are labeled and shown with asterisks. $\Delta\Omega$ grows with more rapid rotation in hydrodynamic cases. Cases labeled a and b sample more turbulent states. (*b*) Kinetic energy of the meridional circulations MCKE, normalized to that energy in the simulation at the solar rate. MCKE decreases with more rapid rotation; a powerlaw of $\Omega_0^{-0.9}$ is shown for reference. Grey dashed lines indicate scalings typically used in mean-field models for more rapidly rotating suns (e.g., [48–50], and see [51] for models that follow the $\Omega_0^{-0.9}$ scaling).

aligned. Correlations in these "bannana-cells" transport angular momentum and build the profile of differential rotation shown in Figure 2*b*; the equator is fast, the poles are slow and the angular velocity contrast is larger than in the Sun. The meridional circulations in contrast are weak and multi-celled in both radius and latitude (Fig. 2*c*). Accompanying the angular velocity profile is a large latitudinal gradient of temperature, shown Figures 2*d*, *e*. Near the surface, there can be 30K contrasts between the hotter poles and cooler mid-latitudes.

The angular velocity contrast of the differential rotation $\Delta\Omega$ and the kinetic energy contained in the meridional circulations (MCKE) is shown for many rapidly rotating suns in Figure 3. Generally, we find that $\Delta\Omega$ grows with more rapid rotation, while MCKE drops strongly [47]. The decrease of MCKE is a surprise and may hold important implications for flux-transport dynamos in the mean-field framework [51]. The growth of $\Delta\Omega$ is roughly in agreement with observations of surface differential rotation in other stars, though substantial disagreement remains between different groups of observers [e.g., 52, 53]. In hydrodynamic cases (triangles) this shear continues to grow with faster rotation; in dynamo cases it may begin to saturate as Lorentz forces become important and react back on the differential rotation (asterisks). In all cases, the growth of $\Delta\Omega$ with rotation rate Ω_0 is accompanied by a growing latitudinal temperature contrast. The temperature contrast grows from a few K at the solar rate to several hundred K at the fastest rotation rates.

The magnetic fields created in dynamo simulations of rapidly rotating suns are organized on global-scales into banded wreath-like structures. These are shown for a dynamo at three times the solar rotation rate (case D3) in Figure 4*a* [54, 55]. Two such wreaths are visible in the equatorial region, spanning the depth of the convection zone and latitudes from roughly $\pm 30°$. The dominant component of the magnetism is the longitudinal field B_ϕ, and the two wreaths have opposite polarities (red, positive; blue, negative). An even more rapidly rotating dynamo (case D5) is shown in Figure 4*b*. Now the wreaths fill the convection zone and the polar caps. These wreaths show significant time-variation and undergo quasi-regular polarity reversals [18].

The time history of these two cases is shown in Figures 5*a*, *b* (case D3 and D5 respectively). Here the mean (axisymmetric) longitudinal magnetic field $\langle B_\phi \rangle$ is shown at mid-convection zone over an interval of about 4000 days; both cases have a full history of roughly 20,000 days.

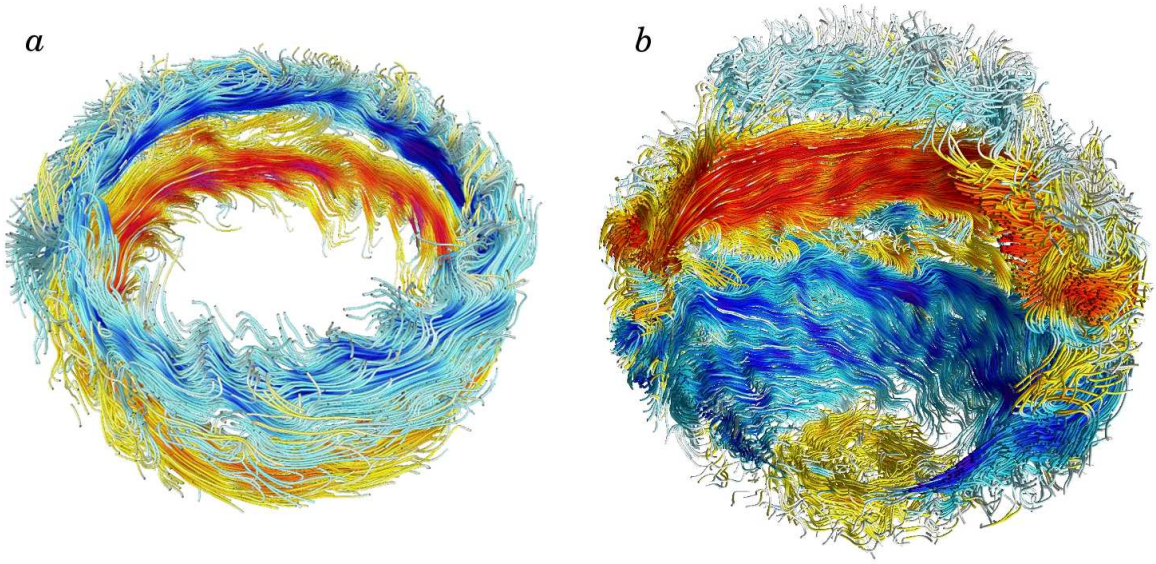

Figure 4. Magnetic wreaths in stellar convection zones. (a) Persistent wreaths in case D3. Two wreaths of opposite polarity (red, positive; blue, negative) form above and below the equator. These magnetic structures coexist with the turbulent convection and retain their identity for more than 20,000 simulated days. (b) Magnetic wreaths in cyclic case D5. In this simulation the wreaths undergo reversals of polarity on roughly a 1500-day timescale. Relic wreaths from the previous cycle are visible in the polar caps. This snapshot is at same instant as Figure 2a.

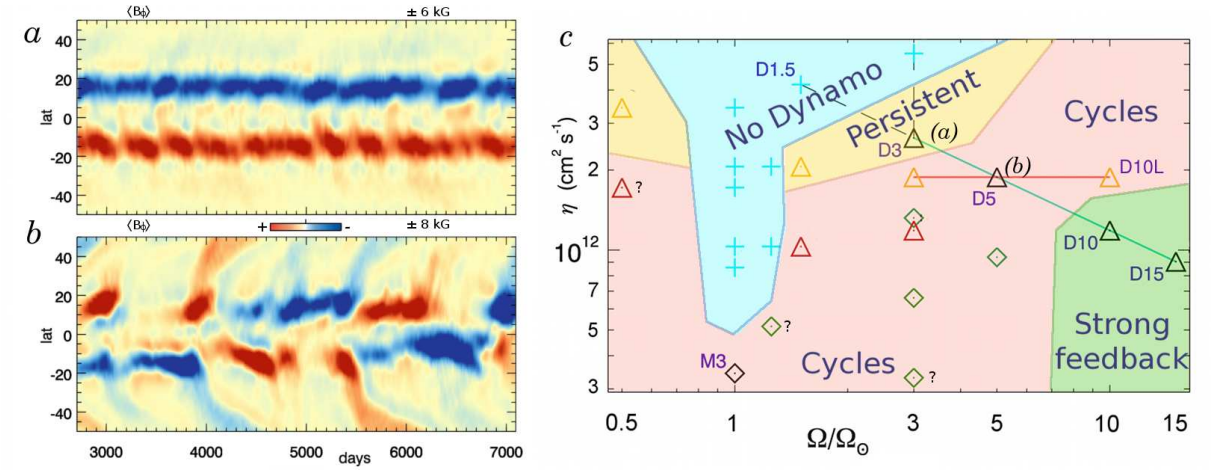

Figure 5. Family of wreath-building dynamo solutions. (a) Time-latitude plot of mean (axisymmetric) longitudinal magnetic field B_ϕ at mid-convection zone in persistent case D3 [55]. (b) Cyclic case D5 shown for same span of time [18]. Three reversals are visible here, occurring on roughly 1500 day periods. (c) Primary control parameters for simulations, with magnetic diffusivity η and rotation rate Ω_0 sampling 0.5–15$\Omega_\odot$. Very approximate dynamo regimes are shown. Time dependence emerges at higher magnetic Reynolds number (lower η) and many dynamos undergo repeated reversals of global-scale polarity. Cases with question marks show significant time-variation but have not been computed for long enough to definitively establish cyclic behavior. At the highest rotation rates the Lorentz force can substantially reduce the differential rotation, but dynamo action is still achieved.

In case D3 we generally find little time variation in the axisymmetric magnetic fields associated with the wreaths; small variations are visible on a roughly 500 day timescale, but the two wreaths retain their polarities for the entire interval, which is significantly longer than the convective overturn time (roughly 10–30 days), the rotation period (9.3 days), or the ohmic diffusion time (about 1300 days at mid-convection zone). We refer to the dynamos in this regime as persistent wreath-builders. Case D5 (Fig. 5*b*) is very different. Here global-scale polarity reversals occur roughly every 1500 days. Three such reversals are shown here. The ohmic diffusion time in this simulation is about 1800 days, while the rotation period is 5.6 days.

These two simulations are part of a much larger family of wreath-building dynamos, which are summarized in Figure 5*c*. Shown here are 26 simulations at rotation rates ranging from 0.5 $\Omega_\odot$ to 15 $\Omega_\odot$. Wreath-building dynamos are achieved in most simulations (17), though a smaller number do not successfully regenerate their mean poloidal fields (9, indicated with crosses). At individual rotation rates (e.g., $3\Omega_\odot$), further simulations explore the effects of lower magnetic diffusivity η and hence higher magnetic Reynolds numbers. Some of these follow a path where the magnetic Prandtl number Pm is fixed at 0.5 (triangles) while others sample up to Pm=4 (diamonds). Near the onset of dynamo action the wreaths are similar to those found in case D3 and persist for long intervals with little variation in time. At higher magnetic Reynolds numbers (lower η and higher Ω_0) we find many simulations that show cyclic reversals of global-scale magnetism (as in case D5). It is difficult to determine what sets the cycle period in these dynamos: cycles appear to become shorter as η decreases, opposite to what might be expected if the ohmic time determined the cycle period. The dependence of cycle period on Ω_0 is less certain. It is striking that coherent magnetic structures can arise at all in the midst of turbulent convection. We find the combination of global-scale spatial organization and cyclic behavior fascinating, as these appear to be the first self-consistent 3D convective stellar dynamos to achieve such behavior in the bulk of the convection zone rather than relying on a stable tachocline of shear.

6. Where we now stand

This is an exciting time in solar and stellar dynamo theory. Stellar dynamo models have progressed tremendously in the past decade. Mean-field models are reaching a point where credible predictions of upcoming solar cycles can be attempted. Meanwhile, several different 3D simulations using distinctly different codes and assumptions have achieved global-scale magnetism and cyclic behavior in simulations of the solar dynamo [e.g., 19–21, 46, 56]. Global-scale organization and cyclic reversals are being found even in simulations without tachoclines. A major challenge now is to understand why such cycles occur. Significant progress can be made on this problem by translating the results of 3D dynamo models into the language of mean-field theory, measuring difficult to constrain quantities such as α and the turbulent electromotive force (emf) that builds the mean poloidal fields. First attempts at diagnosing these quantities are underway [e.g., 18, 55, 57] but now 3D and mean-field modellers must partner to better understand the cyclic dynamo simulations [e.g., 51, 58]. Such efforts will refine the mean-field models but will also yield crucial insights into the operation of the dynamos within the highly turbulent and time-dependent 3D simulations.

It is also crucial that further observational constraints be provided for such 3D models; here is a brief and biased wish list. In the Sun, some sense of the deep meridional circulations would greatly enhance our confidence in modeling results. In particular, it would be useful to determine whether these circulations are multi-cellular in latitude and radius, or whether one large cell extends from the surface to the tachocline. Simulations generally find that thermal-wind balances arise along with the differential rotation. The amplitude of thermal perturbations at the surface is likely to be quite small, of order 1-10K, but the detection (or non-detection) of such a latitudinal gradient would be very useful. Estimates are beginning to be made based on

simulations [e.g., 40, 42, 59–61] and attempts have been made to observe this profile in the Sun [e.g., 62, and references therein]. Any estimate of the properties of giant cell convection in the Sun would be tremendously useful as well. Direct detection of these structures would of course be ideal, but much could be learned from indirect observations as well [e.g., 63].

Convective dynamo models in 3D are being applied to other stars, both similar to and different from the Sun. For the solar-type stars, observations of the surface differential rotation $\Delta\Omega$, its variation with stellar mass and rotation rate, and its temporal variation would greatly constrain these models. Additionally, it is crucial to know how basic dynamo properties, such as the amount of surface magnetism and the cycle period, scale with differential rotation $\Delta\Omega$ rather than overall rotation rate Ω_0. The thermal wind balances achieved in more rapidly rotating solar-type stars likely lead to latitudinal temperature contrasts of several hundred K; in more massive and luminous F-type stars, these contrasts may be as large as several thousand K (K. Augustson, private communication). These signatures may be observable.

The research on wreath-building dynamos in rapidly rotating suns has been done in collaboration with Matthew K. Browning, Allan Sacha Brun, Mark S. Miesch, Nicholas J. Nelson and Juri Toomre. I owe them a great debt of gratitude. I also thank Ellen Zweibel and Cary Forest for inspiring the discussion of η and plasma transport. Funding for this research is provided in part through NSF Astronomy and Astrophysics postdoctoral fellowship AST 09-02004. CMSO is supported by NSF grant PHY 08-21899. The simulations were carried out with NSF PACI support of NICS, PSC, SDSC, and TACC.

References

[1] Pizzolato N, Maggio A, Micela G, Sciortino S and Ventura P 2003 *A&A* **397** 147–157
[2] Baliunas S L et al. 1995 *ApJ* **438** 269–287
[3] Oláh K et al. 2009 *A&A* **501** 703–713 (*Preprint* 0904.1747)
[4] Rempel M 2008 *Journal of Physics Conf. Series* **118** 012032.1–012032.10
[5] Lanza A F 2010 *IAU Symposium*, vol 264, ed A G Kosovichev et al. pp 120–129
[6] Dikpati M and Gilman P A 2006 *ApJ* **649** 498–514
[7] Muñoz-Jaramillo A, Nandy D and Martens P C H 2009 *ApJ* **698** 461–478 (*Preprint* 0811.3441)
[8] Wang Y and Sheeley Jr N R 1991 *ApJ* **375** 761–770
[9] Dikpati M and Charbonneau P 1999 *ApJ* **518** 508–520
[10] Küker M, Rüdiger G and Schultz M 2001 *A&A* **374** 301–308
[11] Nandy D and Choudhuri A R 2001 *ApJ* **551** 576–585 (*Preprint* arXiv:astro-ph/0107466)
[12] Rempel M 2006 *ApJ* **647** 662–675 (*Preprint* arXiv:astro-ph/0604446)
[13] Jouve L and Brun A S 2007 *A&A* **474** 239–250 (*Preprint* 0712.3200)
[14] Yeates A R, Nandy D and Mackay D H 2008 *ApJ* **673** 544–556 (*Preprint* 0709.1046)
[15] Charbonneau P 2010 *Living Reviews in Solar Physics* **7** 3:1–91
[16] Brandenburg A and Subramanian K 2005 *Phys. Rep.* **417** 1–4 (*Preprint* arXiv:astro-ph/0405052)
[17] Jouve L et al. 2008 *A&A* **483** 949–960
[18] Brown B P, Miesch M S, Browning M K, Brun A S and Toomre J 2010 *ApJ* submitted
[19] Ghizaru M, Charbonneau P and Smolarkiewicz P K 2010 *ApJ* **715** L133–L137
[20] Käpylä P J, Korpi M J, Brandenburg A, Mitra D and Tavakol R 2010 *Astr. Nachr.* **331** 73–81
[21] Mitra D, Tavakol R, Käpylä P J and Brandenburg A 2010 *ApJ* **719** L1–L4 (*Preprint* 0901.2364)
[22] Rüdiger G, von Rekowski B, Donahue R A and Baliunas S L 1998 *ApJ* **494** 691–699
[23] Küker M and Stix M 2001 *A&A* **366** 668–675
[24] Küker M and Rüdiger G 2005 *A&A* **433** 1023–1030 (*Preprint* arXiv:astro-ph/0409246)

[25] Küker M and Rüdiger G 2005 *Astron. Nachr.* **326** 265–268 (*Preprint* arXiv:astro-ph/0504411)
[26] Küker M and Rüdiger G 2008 *Journal of Physics Conf. Series* **118** 012029.1–012029.8
[27] Dikpati M, Gilman P A and MacGregor K B 2006 *ApJ* **638** 564–575
[28] Gilman P A 1983 *ApJS* **53** 243–268
[29] Glatzmaier G A 1984 *Journal of Computational Physics* **55** 461–484
[30] Glatzmaier G A 1985 *ApJ* **291** 300–307
[31] Rieutord M and Rincon F 2010 *Living Reviews in Solar Physics* **7** 2:1–82 (*Preprint* 1005.5376)
[32] Braginskii S I 1965 *Reviews of Plasma Physics* **1** 205–311
[33] Rieutord M 2008 *Comptes Rendus Physique* **9** 757–765
[34] Brun A S, Miesch M S and Toomre J 2004 *ApJ* **614** 1073–1098
[35] Clune T L, Elliott J R, Glatzmaier G A, Miesch M S and Toomre J 1999 *Parallel Comp.* **25** 361–380
[36] Miesch M S, Elliott J R, Toomre J, Clune T L, Glatzmaier G A and Gilman P A 2000 *ApJ* **532** 593–615
[37] Nordlund Å, Stein R F and Asplund M 2009 *Living Reviews in Solar Physics* **6** 2:1–116
[38] Brun A S and Toomre J 2002 *ApJ* **570** 865–885 (*Preprint* arXiv:astro-ph/0206196)
[39] Miesch M S 2005 *Living Reviews in Solar Physics* **2** 1:1–139
[40] Miesch M S, Brun A S, DeRosa M L and Toomre J 2008 *ApJ* **673** 557–575
[41] Rempel M 2005 *ApJ* **622** 1320–1332 (*Preprint* arXiv:astro-ph/0604451)
[42] Miesch M S, Brun A S and Toomre J 2006 *ApJ* **641** 618–625
[43] Browning M K, Miesch M S, Brun A S and Toomre J 2006 *ApJ* **648** L157–L160 (*Preprint* arXiv:astro-ph/0609153)
[44] Browning M K, Brun A S, Miesch M S and Toomre J 2007 *Astr. Nachr.* **328** 1100–1103
[45] Miesch M S, Browning M K, Brun A S, Toomre J and Brown B P 2009 *Astro. Soc. of the Pacific Conf. Series*, vol 416, ed M Dikpati et al. pp 443–452 (*Preprint* 0811.3032)
[46] Miesch M S, Brown B P, Browning M K, Brun A S and Toomre J 2010 *Preprint* 1009.6184
[47] Brown B P, Browning M K, Brun A S, Miesch M S and Toomre J 2008 *ApJ* **689** 1354–1372 (*Preprint* 0808.1716)
[48] Charbonneau P and Saar S H 2001 *Magnetic Fields Across the Hertzsprung-Russell Diagram* (*Astro. Soc. of the Pacific Conf. Series* vol 248) ed Mathys G et al. pp 189–198
[49] Dikpati M, Saar S H, Brummell N and Charbonneau P 2001 *Magnetic Fields Across the Hertzsprung-Russell Diagram* (*Astro. Soc. of the Pacific Conf. Series* vol 248) ed Mathys G et al. pp 235–238
[50] Nandy D 2004 *Sol. Phys.* **224** 161–169
[51] Jouve L, Brown B P and Brun A S 2010 *A&A* **509** A32:1–11 (*Preprint* 0911.1947)
[52] Donahue R A, Saar S H and Baliunas S L 1996 *ApJ* **466** 384–391
[53] Barnes J R, Cameron A C, Donati J F, James D J, Marsden S C and Petit P 2005 *MNRAS* **357** L1–L5 (*Preprint* arXiv:astro-ph/0410575)
[54] Brown B P, Browning M K, Brun A S, Miesch M S, Nelson N J and Toomre J 2007 *American Institute of Physics Conf. Series* vol 948 pp 271–278
[55] Brown B P, Browning M K, Brun A S, Miesch M S and Toomre J 2010 *ApJ* **711** 424–438
[56] Nelson N J, Brown B P, Browning M K, Brun A S, Miesch M S and Toomre J 2010 *Preprint* 1010.6073
[57] Racine E, Charbonneau P, Ghizaru M, Bouchat A and Smolarkiewicz P K 2010 *ApJ* submitted
[58] Miesch M S 2008 *Journal of Physics Conf. Series* **118** 012031.1–012031.10
[59] Balbus S A, Bonart J, Latter H N and Weiss N O 2009 *MNRAS* **400** 176–182 (*Preprint* 0907.5075)
[60] Balbus S A and Latter H N 2010 *MNRAS* **407** 2565–2574 (*Preprint* 1005.5100)
[61] Brun A S, Antia H M and Chitre S M 2010 *A&A* **510** A33:1–7 (*Preprint* 0910.4954)
[62] Rast M P, Ortiz A and Meisner R W 2008 *ApJ* **673** 1209–1217 (*Preprint* 0710.3121)
[63] Hanasoge S M, Duvall T L and DeRosa M L 2010 *ApJ* **712** L98–L102 (*Preprint* 1001.4508)